Fine Modulation in Network Activation during Motor Execution and Motor Imagery

Ana Solodkin, Petr Hlustik, E. Elinor Chen and Steven L. Small

Department of Neurology and Brain Research Imaging Center, The University of Chicago, Chicago, IL 60637, USA

Motor imagery, the 'mental rehearsal of motor acts without overt movements', involves either a visual representation (visual imagery, VI) or mental simulation of movement, associated with a kinesthetic feeling (kinetic imagery, KI). Previous brain imaging work suggests that patterns of brain activation differ when comparing execution (E) with either type of imagery but the functional connectivity of the participating networks has not been studied. Using functional magnetic resonance imaging (fMRI) and structural equation modeling, this study elucidates the inter-relationships among the relevant areas for each of the three motor behaviors. Our results suggest that networks underlying these behaviors are not identical, despite the extensive overlap between E and KI. Inputs to M1, which are facilitatory during E, have the opposite effect during KI, suggesting a physiological mechanism whereby the system prevents overt movements. Finally, this study highlights the role of the connection of superior parietal lobule to the supplementary motor area in both types of motor imagery.

Keywords: functional imaging, motor circuits, motor imagery, network analysis, structural equation modeling

Introduction

Studies in systems neuroscience are benefiting tremendously from human imaging techniques such as functional magnetic resonance imaging (fMRI). However, image analysis in fMRI has generally focused on enumerating areas of activation under different behavioral conditions, rather than characterizing the networks involved in the generation of those behaviors. Thus, with respect to localizational assumptions, these studies are analogous to lesion analysis studies and incorporate some of the same advantages and limitations. An alternative approach (Gonzalez-Lima and McIntosh, 1994; Buchel and Friston, 1997, 2000; Horwitz *et al.*, 2000; Taylor *et al.*, 2000) involves assessing networks of activation and the effective connectivity among areas activated during different behavioral conditions. These models offer an interesting new perspective on experimental design and data analysis by providing an analytical approach to understanding integrated systems.

Following their lead, the present paper describes effective connectivity in networks associated with three different hand motor conditions: execution of hand movements (E) and kinetic and visual imagery of these same movements (KI and VI). This work was motivated in part by reports suggesting a possible role of 'motor imagery' in the improvement of motor skill in normal subjects and in recovery after neurological damage. In normal subjects, for instance, motor imagery is used by athletes and professional musicians, where it is called 'mental rehearsal', to improve performance. By the same token, motor imagery is used therapeutically after stroke to stimulate recovery of motor abilities (Warner and McNeill, 1988; Ryding *et al.*, 1993; Yaguez *et al.*, 1998, 1999).

In the most general sense, motor imagery refers to the 'mental rehearsal of simple or complex motor acts that is not accompanied by overt body movements' (Jeannerod, 1995; Porro *et al.*, 1996).

Although the definition appears simple, people asked to perform motor imagery do not make an unambiguous interpretation unless instructed more specifically. In particular, people ordinarily perform this mental rehearsal of movements according to one of two strategies, as follows. (i) they produce a visual representation of their moving limb. In this case, the person is a spectator of the movements (external imagery). We will refer to this behavior as visual imagery (VI). (ii) People mentally simulate the movements associated with a kinesthetic feeling of the movement. In this case, the person is a performer (internal imagery). We will refer to this behavior as kinetic imagery (KI).

In fact, each of these strategies of motor imagery has different properties. While KI is difficult to verbalize, VI is not. Whereas KI follows Fitt's law (i.e. the imagined movement associated with KI shows the same limitations as movements during execution), VI does not. This means that during KI, a person cannot perform movements at a higher rate than during overt execution and this still holds after brain injury, when both execution and KI are diminished correspondingly. By contrast, during VI, a person can imagine movements that exceed the physiological limitations of the execution (for a review, see Jeannerod, 1995). Moreover, certain physiological changes associated with KI mimic those occurring during execution, whereas during VI, they do not. For example, electromyographic (EMG) activity during KI shows an increase in voltage in the muscles corresponding to movement execution, but there are no such changes during VI (Fadiga *et al.*, 1999). Furthermore, the excitability of the cortico-spinal system measured with transcranial magnetic stimulation is increased during KI but not VI (Stephan and Frackowiak, 1996; Abbruzzese *et al.*, 1999; Fadiga *et al.*, 1999; Hashimoto and Rothwell, 1999; Rossini *et al.*, 1999). In addition, if these imagery tasks involve strenuous movements, KI (but not VI) will show concomitant changes in autonomic function similar to those present during execution, including increases in heart and respiratory rates as well as in end-tidal PCO_2 (Decety *et al.*, 1991; Oishi *et al.*, 1994, 2000).

Since KI shares more physiological characteristics with the movement execution than does VI, it has been associated more closely with motor functions *per se* such as motor preparation, imitation and anticipation, and the refining of motor abilities (Stephan and Frackowiak, 1996; Deiber *et al.*, 1998; Fadiga *et al.*, 1999; Jeannerod, 1995; Lotze *et al.*, 1999).

With respect to imaging studies, several accounts of areas activated during KI or VI have been reported using PET or fMRI. Even though some of the studies do not differentiate between KI and VI, there are several features common to most of them (Roland *et al.*, 1980b; Decety *et al.*, 1994; Hallett *et al.*, 1994; Sanes, 1994; Kim *et al.*, 1995; Stephan and Frackowiak, 1996; Lotze *et al.*, 1999; Gerardin *et al.*, 2000; Jeannerod, 2001; Toni *et al.*, 2001). In general, studies have shown that several areas are activated during motor imagery tasks. Included in these active regions are the following: supplementary motor area, superior and inferior parietal lobule, dorsal and ventral lateral pre-motor cortices, pre-frontal areas, inferior frontal gyrus, superior temporal gyrus, primary motor cortex (M1), primary sensory cortex, secondary sensory area, insular cortex, anterior cingulate cortex, superior temporal gyrus, basal ganglia and cerebellum. This extensive activation suggests a complex distributed circuit. In studies that compared execution to motor imagery, it was found that although the areas active tend to be similar between the two conditions, volumes of activation tend to be larger during execution than during motor imagery (Stephan and Frackowiak, 1996; Gerardin *et al.*, 2000; Jeannerod, 2001). A controversial point in some of these studies is the role of M1 during imagery, since its activation is not seen consistently in all studies and if seen, it is less active than during execution (Beisteiner *et al.*, 1995; Fadiga *et al.*, 1999; Hashimoto and Rothwell, 1999; Lotze *et al.*, 1999). The lack of M1 involvement during motor imagery has been explained as the way the system avoids overt movements during imagery.

In summary, previous work suggests that the volume of brain activation differs between execution and motor imagery and that with few exceptions the distribution of activation tends to be similar in the two conditions. Since the patterns of activation are similar, it would be of tremendous interest to determine if the relationships among these areas (effective connectivity) differ between execution and motor imagery (in both kinetic and visual imagery).

The present study addresses this outstanding question. The study addresses first the comparative assessment of areas activated during E, KI and VI. Secondly, the study performs path analysis using structural equation modeling and establishes the inter-relationships among the activated areas for each condition, highlighting the effective connectivity within functional networks.

Materials and Methods

Pilot Study

Before performing the imaging study in the scanner, we measured electromyographic (EMG) activity during execution of unpaced thumb-opposition movement (E) and KI and VI of the movement. Surface electrodes were placed on the first dorsal interosseus (FDI). Signals were recorded using a Biopac 100B amplifier (Santa Barbara, CA). Data were analyzed using conventional FFT and by integrating the signal under the waveform corresponding to each condition. Comparisons of voltage recordings during VI, KI and E were compared using Student's *t*-test.

Imaging Study

The study used blood oxygen level dependent (BOLD) fMRI to map the entire brain (128 × 128 × 24 voxels) at high spatial resolution (1.875 × 1.875 × 6 mm per voxel).

Subjects

Eighteen normal subjects (age range 21–54 years; mean = 30) participated in the study. Four subjects were left-handed and fourteen were right-handed as assessed by the Edinburgh Handedness Inventory (Oldfield, 1971). Nine were females. The study was approved by the Institutional Review Board of the Biological Science Division of the University of Chicago. All subjects understood completely the nature of the experimental procedures and provided written informed consent prior to participation.

Stimulus Presentation

Subjects were divided randomly to either one of two groups: The first group performed kinetic imagery and motor execution and the second group performed visual imagery and motor execution. This design was necessitated by the inherent difficulty for one subject to perform both types of imagery in close temporal proximity to one another. Subjects were placed in the scanner and head movement was restricted with foam rubber pillows. Electrostatic headphones (Resonance Technologies, Northridge, CA) were wrapped around the ears and connected to a stereo system controlled by a Macintosh computer. The computer used the PsyScope psychological software system (Cohen *et al.*, 1993) to present the experimental conditions.

The fingers of the dominant hand were numbered from 1 to 4 (1 = index, 2 = middle, 3 = ring, 4 = pinky). Numbers from 1 to 4 appeared randomly on the screen and for each one, subjects performed the corresponding finger–thumb opposition. The task was externally paced at a rate of 2 Hz. Since this task is not easy to perform at that rate, subjects were trained for 10 min on the execution condition prior to the scanning session. All subjects demonstrated virtually perfect performance before the scan session. The motor task paradigm included one of the two imagery conditions, the execution condition and a rest condition. The motor task described above was followed by a rest condition that required that the subject remain still but view the same random numbers from 1 to 4 on the screen. The onset of each task was signaled with an auditory tone lasting 200 ms. Stimulus presentation was organized in blocks lasting 16 s each, with 32 blocks composing one experimental run. There were four runs. Two execution runs consisted of movement execution blocks alternating with rest blocks (E–R). Two imagery runs consisted of imagery (visual or kinetic) blocks alternating with rest blocks (I–R). The E–R or I–R sequence was repeated 16 times in each run, for a total duration of 8:32 min per experimental run. Each participant performed an execution run first, followed by an imagery run, a second execution run and, finally, a second imagery run.

Imaging

Data acquisition used the spiral k-space method (Noll *et al.*, 1995) on a 1.5 T Signa scanner (GE Medical Systems, Milwaukee, WI) with a standard quadrature GE head coil. Twenty-four contiguous 6 mm axial slices were obtained starting from the vertex through the bottom of the cerebellum. A gradient echo spiral scan pulse sequence used a single spiral to provide 1.875 × 1.875 mm resolution over a 24 cm field-of-view (FOV). T_2^*-weighted imaging was accomplished with a gradient echo time (T_E) of 35 ms, and a repetition time (T_R) of 4000 ms with a flip angle of 60°. A complete set of 24 slice locations was generated every repetition time cycle (4 s). Structural T_1-weighted anatomical images (500 ms T_R, 16 ms T_E, spin echo pulse sequence) were acquired to determine the anatomy of the functional slices. Each of the twenty-four slices was acquired four times during each 16 s active task interval. Since each active task was repeated 16 times during each experimental run, the total number of whole brain images obtained for each active condition for each experimental run was 64. Since each run was repeated twice, there are 128 whole brain images for execution and 128 for imagery. In addition, 64 whole brain images during rest were collected during each run.

Image Analysis

Intra-subject Analysis. Statistical analysis of individual subject data was performed using cross-correlation thresholding (Bandettini *et al.*, 1993; Binder and Rao, 1995). A Monte Carlo simulation was performed to establish the appropriate correlation coefficient to achieve a whole brain alpha <0.05 (Forman *et al.*, 1995). After

enforcing a three-dimensional contiguity requirement in which each cluster of contiguous voxels was constrained to contain at least 9 voxels (~190 mm^3), the appropriate correlation coefficient (r = 0.37) was selected.

Inter-subject Analysis. Multi-subject analysis was performed using a region-of-interest (ROI) approach, based on several specific regions of interest identified a priori in each hemisphere on the basis of the known functional neuroanatomy of the human motor system. The landmarks to delimit the ROIs are summarized in Table 1. Some of these have also been published previously (Solodkin *et al.*, 2001). These areas included the following: M1 (primary motor cortex), S1 (primary and secondary somatosensory cortices), LPMC (lateral pre-motor cortex, dorsal), SMA (supplementary and pre-supplementary motor areas), CMA (cingulate motor area), CRB (cerebellum), PAR (superior parietal lobule and intra-parietal sulcal area), IF (inferior frontal cortex, LPMC ventral; inferior frontal gyrus and anterior insular cortex), OCC (occipital lobe), P/O (parieto-occipital area) and THAL (Thalamus).

The image data were subjected to two complementary analytical approaches. First, analysis involved statistical inferences on the raw data. The main statistical results presented come from an analysis of variance (ANOVA) on the thresholded brain activation volumes to assess differences and statistical interactions among region of interest and task type. This analysis was supplemented by various post-hoc tests (Student–Newman–Keuls). Both the ANOVA and the post-hoc Student–Newman–Keuls statistic were performed in StatView 5.0 for Macintosh (SAS Institute, Cary, NC).

The second analysis involved structural equation modeling (SEM) of the network involved in the execution and imagery circuits. The SEM was performed using the Amos software as described by Arbuckle (1989).

The procedural steps used to assess networks of activation following SEM are explained in some detail, as follows.

1. Determination of an anatomical model. Construction of such a model requires a theoretical anatomical network incorporating 'connection strengths' (regression weights) between the nodes (ROIs) of the model. These theoretical networks must be inferred from data in macaques. In previous studies using SEM, authors (Nyberg *et al.*, 1996; Buchel and Friston, 1997; Kohler *et al.*, 1998) have estimated the connection strengths based on available anatomical data. These values range from 0 to 1.0; however, if no value is chosen, a default value of 0.4 is used. Determination of these theoretical connection strengths can be difficult for two reasons: (i) direct comparison of data across studies is complicated due to differences in techniques and species used and (ii) there can be a mismatch between the anatomical and the physiological strengths of connections (Vanduffel *et al.*, 1997). For these reasons, we decided to approach the issue in a slightly different way estimating physiological strengths of connections following methods described in the Supplementary Data.
2. Generation of the covariance matrix. For each subject, time series values are obtained by averaging the variance of intensities for all active voxels within each ROI.
3. Group analysis. Then a group covariance matrix for all subjects is generated based on an average times series for all subjects for each ROI. Hence, a single network for each condition was generated.
4. Generation of the structural equations. The interregional correlations of activity are used to assign initial numerical weights to the connections (path coefficients) in the anatomical model, leading to the functional model. These equations based on the observed covariance matrix, are a computationally efficient method to solve the path coefficients and will be expressed on the influence of regions on each other (Gonzalez-Lima and McIntosh, 1994; McIntosh and Gonzalez-Lima, 1994; McIntosh, 1999).
5. Solving the equations (AMOS for Windows version 4.0; SmallWaters Corp, Chicago, IL). The equations are solved simultaneously using an iterative maximum likelihood method to obtain an optimal value for each connection that represents the effective connectivity from each pair of ROIs (nodes). The notion is that the effective connectivity value will reflect the amount of influence that the output area has on the input area. The best solution to the set of equations will minimize the differences between the observed and the predicted covariance matrices.
6. Goodness of fit between the predicted and observed variance matrices. The next step in the use of the model includes the use of goodness-of-fit statistics using χ^2 distribution with $q(q + 1)/2 - p$ degrees of freedom (where q is the number of ROIs and p is the number of unknown coefficients). If the null hypothesis is not rejected, it means a good fit was obtained.
7. Comparison among different networks. Group networks from each condition (E, KI and VI) are compared using the stacked model (Gonzalez-Lima and McIntosh, 1994; McIntosh and Gonzalez-Lima, 1994; McIntosh *et al.*, 1994). In the stacked model, the two networks

Table 1
Anatomical description of the cortical regions of interest

ROI	Areas included	Brodmann's	Delimiting landmarks
M1	Primary motor cortex	4	Anterior bank of central sulcus; A = posterior edge of precentral gyrus
S1	Primary and secondary sensory areas	1, 2, 3, 5	A = central sulcus; P = post-central sulcus
LPMC	Lateral pre-motor cortex, dorsal	6l	A = vertical plane through anterior commissure; P = M1; I = inferior frontal sulcus
SMA	Supplementary and pre-supplementary motor areas	6m	A = vertical plane through genu of corpus callosum; P = paracentral lobule; I = CMA
CMA	Cingulate motor area	23c and 24c	Both banks of the cingulate sulcus; A = vertical plane through the genu of the corpus callosum; P = vertical plane through the splenium of the corpus callosum
PAR	Superior parietal lobule and intraparietal sulcus	7	A = post-central sulcus; P = line between parieto-occipital sulcus and occipital notch; I = inferior bank of intra-parietal sulcus
IF	Inferior frontal gyrus, vLPMC, anterior insula	6l, 44, 45, 14	A = lateral orbital sulcus; P = pre-central sulcus; S = inferior frontal sulcus; M = anterior short insular gyrus
T/O	Temporo-occipital area	36	A = vertical plane through lat. geniculate; P = line between occipital notch and splenium of the corpus callosum; I = collateral sulcus
P/O	Parieto-occipital area	20, 39, 40	A = inferior post-central sulcus; P = line between parieto-occipital sulcus and occipital notch; S = inferior bank of intra-parietal sulcus; I = line from ascending lateral sulcus to lateral occipital sulcus
OCC	Occipital lobe	17, 18, 19	M = parieto-occipital sulcus and cingulate sulcus; L = line between the parieto-occipital sulcus and the occipital notch

All cortical regions considered in this study are listed in the table by the acronyms used (first column), the specific regions included in each ROI (second column), the corresponding Brodmann area (third column) and the anatomical and imaginary landmarks used to delimit each ROI on each individual brain (fourth column). A, anterior limit; P, posterior; I, inferior; S, superior; M, medial; L, lateral.

to compare are combined in a single program run. The process involves statistically comparing networks with constrained path coefficients (null model) with those where the coefficients are allowed to differ (alternative model). The difference between models is quantified by the χ^2 difference between the null-model and the alternative model. If the χ^2 difference is significantly larger than the difference in the degrees of freedom, the null model is rejected, implying that the networks from each condition are different. The stacked model requires identical anatomical models. Since there were fewer areas active for the imagery conditions than for execution, we obtained these missing nodes from a random and constant time series vector from the corresponding ROI. The missing path coefficients were fixed to a value of zero.

There are some limitations associated with SEM, as follows.

1. It does not lead to a unique solution. One of the main criticisms of SEM is that solutions will be different depending on the theoretical model used and that these could vary widely. However, it is possible to start with simple models and then progress to more complex theoretical models, since the goodness of fit is a sensitive measure to determine how well the theoretical model adapts to the actual data. In addition, we consider not only goodness of fit for the final model, but also reliability of connections and residual values to determine the strength of our final model.
2. If two regions have a correlation close to 1.0, the system groups them into a single area. This limitation comes from the software rather than the model. However, in our experience, this case has only occurred when movement artifact is present providing a DC offset which increases the correlation values.
3. It can be very sensitive to motion artifacts that can produce false positive correlations. To avoid this problem, we review case-by-case complete time series in order to detect these movement artifacts and then correct them.

Results

Pilot Study

EMG Recording during Execution and Imagery

The EMG recordings in the first dorsal interosseus (FDI) during execution and kinetic and visual imagery tasks were associated with different responses. During execution, clear muscle spindles were recorded, which were absent during either KI or VI (Fig. 1). However, the activation during the two types of imagery was not similar: the amplitude of the signal during kinetic imagery was larger than during visual imagery, and the frequency was higher. The pattern during VI did not differ from rest. These initial results were essential for the imaging study, since it was the only way to gauge the subjects' ability to perform the required task and to monitor task performance, even though this had to be outside the scanner room prior to the scan session.

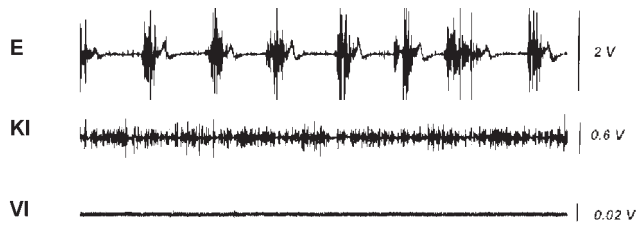

Figure 1. Electromyographic recordings during E, KI and VI. The upper trace shows EMG activation in the FDI during finger opposition movements. The second trace during KI and the third trace during VI. Muscle tone increased during KI but not during VI which did not differ from rest.

Brain Imaging Results

Volumes of Activation (Table 2 and Fig. 2)

During the execution task, several areas were active in all subjects. These areas included M1, S1, superior parietal lobule (PAR), dorsal lateral premotor cortex (LPMC), supplementary motor areas (SMA) and cerebellum (CRB). Occipital areas were also commonly active (OCC). In addition to these areas, several other areas showed clusters of activation in some, but not all subjects. Among these areas, the following were most prominent: inferior frontal gyrus (IF), medial frontal areas, thalamus, temporo-parietal areas (T/P) and temporo-occipital areas (T/O). The kinetic imagery task showed activation in the following: LPMC, M1, S1 (mostly S1 proper), SMA, CRB and PAR. Activation in the OCC area as well as the T/P area, THAL and IF areas were also seen, although they were not present in all subjects. During visual imagery, the relevant areas included: LPMC, PAR, SMA, OCC, CRB and occasionally, IF areas.

Analysis of variance (ANOVA) performed on volumetric values of brain activation showed a significant primary effect of task ($F = 13.699$, $P < 0.0001$) and a significant primary effect of region ($F = 9.935$, $P < 0.0001$). In addition, there was a significant interaction between task × region ($F = 1.655$, $P = 0.0426$). *Post hoc* analysis of the primary effects showed that the execution condition was associated with a significantly larger volume of activation ($P < 0.0001$) than the imagery conditions, whereas there was no significant difference in volumes between the kinetic and visual imagery tasks.

Although the primary effect volumes of activation during execution were larger than during imagery, not all ROIs showed a significant difference. *Post hoc* analysis of the task × region interaction showed a significant effect in a number of ROIs in three different patterns, as follows.

1. The total volume of activation in CRB was larger during execution than during visual or kinetic imagery.
2. The volume of activation in the IF areas was larger during execution than during kinetic imagery but not during visual imagery.
3. The volume of activation in LPMC, M1, S1, SMA and PAR was larger during execution than during visual imagery, but not

Table 2
Mean volumes of activation (mm^3) ± SE per region

	Execution	Kinetic imagery	Visual imagery
CRB	1281 ± 269	336 ± 252	147 ± 104
IF	294 ± 102	21 ± 21	42 ± 21
M1	1911 ± 458	735 ± 308	0 ± 0
LPMC	2058 ± 555	1197 ± 311	567 ± 153
S1	714 ± 185	315 ± 189	42 ± 21
SMA	588 ± 123	525 ± 105	147 ± 41
PAR	1512 ± 241	924 ± 231	441 ± 145
OCC	672 ± 228	189 ± 145	609 ± 438
T/P	147 ± 83	21 ± 21	0 ± 0
THAL	42 ± 21	0 ± 0	0 ± 0

For each ROI, this table shows the mean volume of activation (mm^3) ± standard error during each behavioral condition. To convert to voxels of activation, divide by the voxel size ($1.875 \times 1.875 \times 6mm = 21mm^3$).

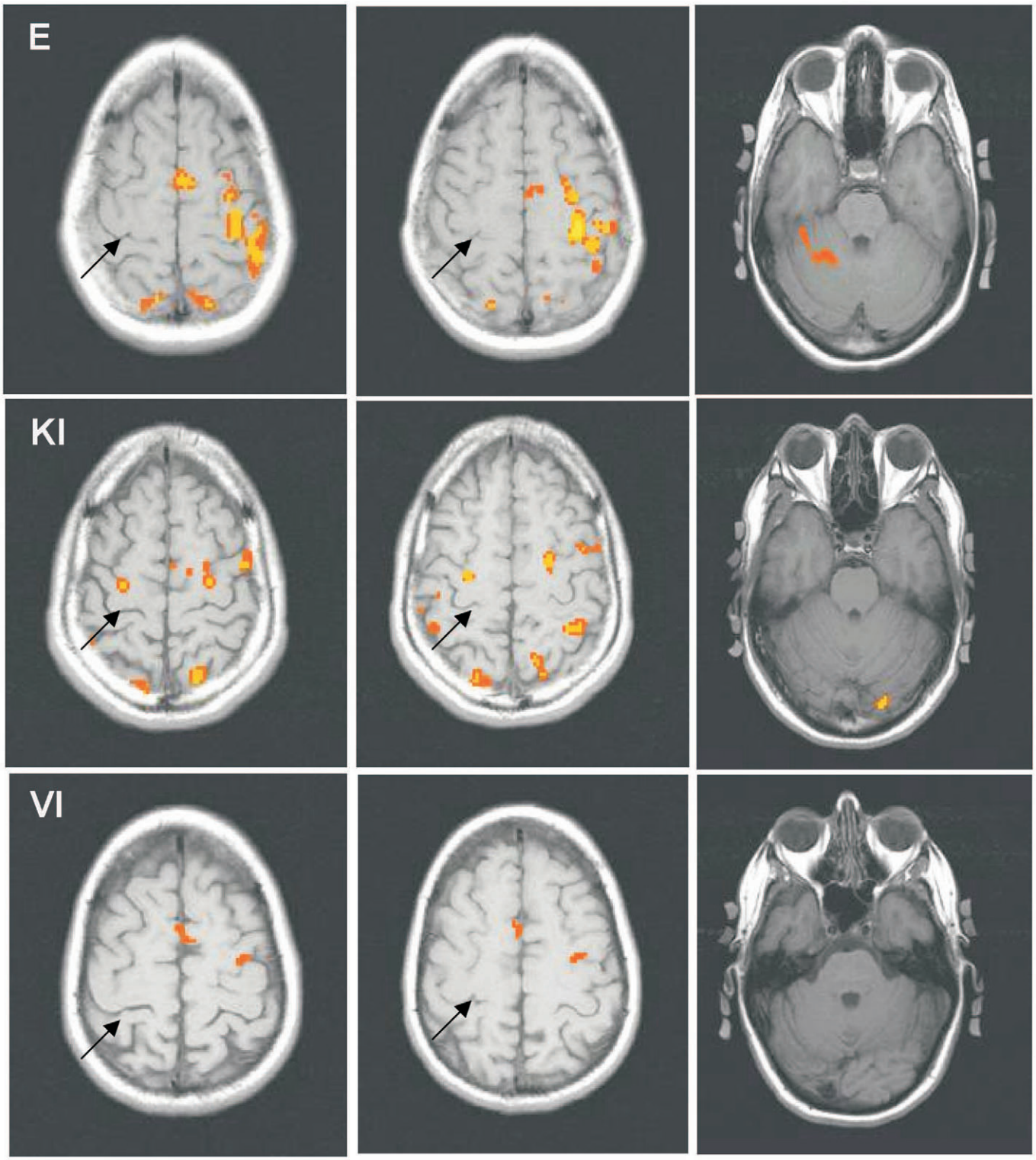

Figure 2. Single subject fMRI during E, KI and VI. Brain activation was seen in several sensory and motor areas during E (upper panels), KI (middle panels) and VI (lower panels). The first and second columns of these axial slices depict regions at the level of the hand motor area of M1. For orientation purposes, the arrows are pointing to the central sulcus. The third column represents axial slices at the level of the cerebellum. Note that volumes of activation were much larger during E than during KI or VI. Since these are radiological images, the left side of the figure represents the right hemisphere.

kinetic imagery.

4. The volumes of activation in other areas (T/O, T/P and THAL) did not differ across any of the three conditions. Table 2 shows the volumetric values for each condition.

Network Analysis

Figure 3 shows the final network depicting effective connectivity for each of the three conditions. Note that the a priori biological model incorporated physiological connection

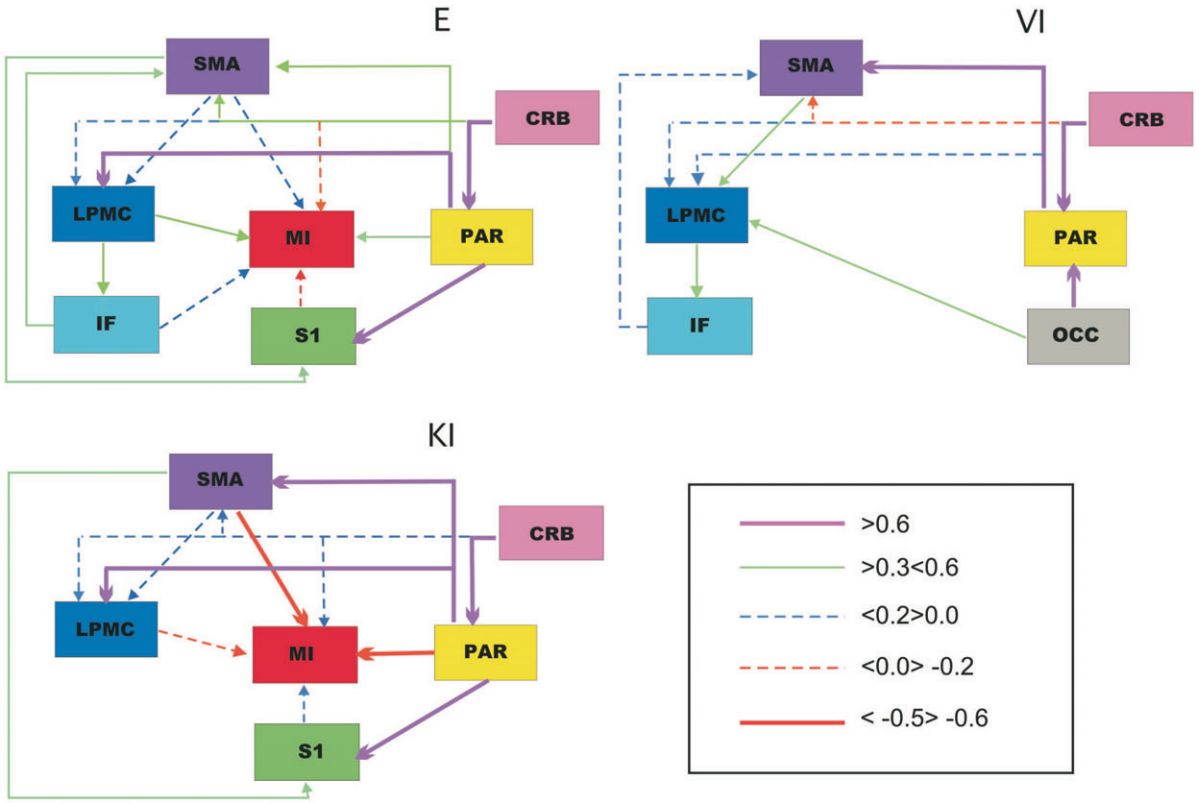

Figure 3. Final networks for E, KI and VI. This figure depicts the values of effective connections during the three experimental conditions. Note the close parallels between E and KI except in the connections between association motor areas and superior parietal lobule with M1. In contrast, the patterns of connectivity in the VI conditions were biased towards visual areas.

strengths (as described in the Supplementary Data), rather than the evaluation of pathway strengths based on anatomical data or the use of default values. Since our method for assessing physiological strength is not the norm for previous studies using path analysis, we ran the model twice, once using default values (0.4) and once using our 'physiological' values (see Supplementary Data). Although, these manipulations led to a difference in the absolute connection strengths in the final models, the relative difference among the connection strengths in the models did not change except in the low range. These latter values tended to be higher using the default scheme than the derivational one, leading to less spread among the values. Since the physiological strength values provided a more sensitive measure, the final model is based on theoretical anatomical model that incorporates the physiological connection strengths.

Values of effective connectivity. During E, effective connectivity to M1 tended to be strongest from LPMC and PAR, whereas the effective connectivity from SMA, S1, CRB and IF tended to be weaker. In addition, strong connections were seen between PAR and LPMC and S1, and from CRB to PAR. During KI, all outputs from PAR (to S1, M1, SMA and LPMC) were very strong as was the connection from CRB to PAR. The effective connectivity to M1 was strong from PAR and SMA, and weak from LPMC, CRB and S1. The network for VI showed predominance of the connections involving OCC areas (to PAR and LPMC) as well as the connection between CRB to PAR.

In summary, E and KI seem to be closely related tasks, since they share several, identical parts of the network (PAR to LPMC and S1; CRB to M1, LPMC and PAR; SMA to LPMC). The VI condition differs the most. In addition, in the two imagery conditions the inputs to SMA from PAR and CRB did not vary. On the other hand, the connections between CRB to PAR and LPMC were constant in the three conditions.

Goodness of fit. The χ^2 values for each condition were as follows: execution, $\chi^2 = 8$, df = 4, $P > 0.05$; kinetic imagery, $\chi^2 = 6$, df = 2, $P > 0.05$; visual Imagery, $\chi^2 = 11$, df = 5, $P > 0.05$. These results indicate that there is no significant difference ($P > 0.05$) between the theoretical (anatomical) and the analytical (experimental) models (null hypothesis is not rejected). The solution to the structural equations is a good fit.

Residual effects. Most ROIs had residual values <5%, which means that 95% of the variance in each region is explained by the variability in activation from input areas. The only two exceptions are SMA and IF regions, which had residual values ≈50%. The higher residual values in these two regions could be explained by missing inputs from the model or could reflect complex intrinsic connectivity within these areas (McArdle and McDonald, 1984; McIntosh and Gonzalez-Lima, 1992).

Reliability of effective connectivity values. Since our final model describes a group network, we calculated the standard deviation of the effective connectivity values. In the E condition, the effective connectivity values from CRB to LPMC, to SMA and to M1 had high standard deviations, reflecting more variable results. Since all include CRB, the source of this

variability could be due to the fact that we are missing the link from CRB to cerebral cortex via thalamus even though indirect connections can be assessed with structural equation modeling (McIntosh and Gonzalez-Lima, 1994).

Comparison between networks. This was performed using the stacked model (Gonzalez-Lima and McIntosh, 1994; McIntosh and Gonzalez-Lima, 1994; McIntosh *et al.*, 1994). We made two comparisons. (i) Comparison between the E conditions across the two groups of subjects gave a χ^2 difference = 1.59, df = 5, P = 0.90, indicating that the networks are not significantly different. It was thus concluded that both groups of subjects belong to comparable populations. (ii) Comparison between the network for execution and that for kinetic imagery gave a χ^2 difference = 122, df = 17, $P < 0.005$; this is in contrast with the comparison between visual imagery and execution, which gave a χ^2 difference = 449, df = 19, $P < 0.001$. This indicates that both imagery networks are significantly different from the network for the execution task.

When comparing the networks for E to the network for KI, there are few differences. First in KI, the path coefficients from LPMC to IF and from IF to M1 are non-existent during KI. Secondly, there are remarkable differences in the values of effective connectivity for the inputs to M1. First, the influence of LPMC was reduced and changed from positive to negative. Whereas the input from SMA radically increased, the input from PAR increased to a lesser extent. As with the input from LPMC, inputs from SMA and PAR also changed sign, from positive to negative. The inputs from S1 and CRB did not change their weak strength but did change from negative to positive.

The network for VI was significantly different from the network for E. First, all connectivity values involving M1 and S1 were absent. Secondly, while the path coefficient between SMA and LPMC increased slightly, effective connectivity values were strong between OCC areas and PAR (very strong) and from OCC to LPMC (less strong). In other words, the most relevant path coefficients during VI were biased towards OCC areas.

Discussion

Comparison with Previous Studies

In general terms, the present study largely confirmed the functional anatomy of motor imagery as enumerated in the introduction. Some exceptions were found. The present study did not find activation during motor imagery in the cingulate cortices, including both cingulate motor and limbic areas (Decety and Jeannerod, 1995; Stephan and Frackowiak, 1996; Crammond, 1997; Deiber *et al.*, 1998), or in the prefrontal areas (BA 44; Gerardin *et al.*, 2000). The reasons for this small discrepancy in terms of CMA could be attributable to the fact that in previous studies, the areas of activation were localized using a linear transformation into the Talairach stereotactic space (Talairach and Tournoux, 1988). The spatial distortion introduced by this transformation is exacerbated in studies presenting group average data. If such distortion had not been introduced in these analyses, their results could coincide with our observations and those of others (Paus *et al.*, 1996; Machulda *et al.*, 2001; Rademacher *et al.*, 2001, 2002). The reason of the discrepancy with other studies that showed activation of prefrontal regions (especially area 44), could be that we did not use a goal-directed motor task. As Binkofski *et al.* (2000) have suggested, the activation of this area during motor imagery is only present with goal-oriented motor tasks and not with other movements.

Most previous studies find that the volumes of activation in the primary motor cortex during execution are larger than that seen during kinetic imagery (Jeannerod, 1995; Kim *et al.*, 1995; Stephan and Frackowiak, 1996; Lotze *et al.*, 1999). In the present study, indeed the volumes of activation in M1 tended to be smaller during the KI condition than the E condition even though there was not a statistically significant difference. This was a general trend for all areas during the imagery tasks. In contrast to the previous studies, which highlight this fact and relate it to the lack of overt movement, the present work finds an explanation in changes in the interrelationships among areas across the three conditions.

Network Analysis

The description of brain imaging data using structural equation modeling (Gonzalez-Lima and McIntosh, 1994; Buchel and Friston, 1997, 2000; Horwitz *et al.*, 2000; Taylor *et al.*, 2000) has produced a conceptual change in the way we interpret such data. In particular, by determining networks of activation, SEM describes the functional influences among anatomical brain regions. The emphasis thereby changes from the individual brain regions active in each condition to the relationships among them. In the past, McIntosh and his collaborators (McIntosh, 1999, 2000; McIntosh *et al.*, 2001) have referred to this modulation of functional connectivity as 'neural context'. The results of the present study demonstrate that independent of the volumes of activation *per se*, clear differences (and similarities) exist in the networks for E, KI and VI.

The Networks for E, KI and VI were Statistically Different

Our results showed that the networks for the two imagery conditions differ when each is compared to the network for the execution condition. Since the stacked method requires that similar brain areas be included within the compared networks (see Materials and Methods), any observed differences should be due to differences in connectivity. The difference between KI and E is of special interest because they share several common elements. With the exception of IF, the areas active during E and KI were similar as were several of the connectivity values (PAR to LPMC and to S1; S1 to M1; SMA to LPMC and CRB to M1 and LPMC). These parallels suggest that influences among areas involved in sensory-motor integration are kept constant during E and KI. Thus during KI and E, not only are similar areas active, but the relative influence of these areas on each other also remains constant. This notion reinforces further the idea of KI as a true motor behavior, a postulate also supported by behavioral data, since KI has been associated with motor preparation, imitation and anticipation, motor restraint, motor execution and motor learning (Jeannerod, 1995; Stephan and Frackowiak, 1996; Deiber *et al.*, 1998; Fadiga *et al.*, 1999; Lotze *et al.*, 1999).

The most notable differences among the networks for KI and E were found in the inputs to M1. During KI, concomitant with the decrease in the influence of LPMC on M1, was an increase in the extent of the influence of both SMA and PAR on M1. Furthermore, by contrast with the weak positive influence these areas have on M1 during E, their influence during KI was strong and negative. These negative values could be interpreted as a suppression effect (McIntosh and Gonzalez-Lima,

1994, 1998) of SMA and PAR on M1, since during KI there are no overt movements. We call it a suppressive effect rather than inhibition in the classic physiological sense because with fMRI, both inhibitory and excitatory influences are detected with the BOLD response (Waldvogel *et al.*, 2000; Attwell and Iadecola, 2002). However, the fact that these connectivity values change from weak and positive to strong and negative during a task with no overt movements (KI) provides a new perspective on how the motor system might be encoding information. In other words, we have two closely related tasks (E and KI), involving activation in similar areas, and with several similar interrelationships. Yet even when the volumes of activation in M1 during KI are much smaller, the influence exerted by SMA and PAR is opposite their influence during E. This exemplifies how network analysis can provide a new perspective on the neurophysiology of the motor system by describing how changes in the interrelationships among areas can generate different motor behaviors.

One outstanding question involves the possible cortical origin of the increase of muscle tone during KI (and not VI). In previous reports (Stephan and Frackowiak, 1996; Abbruzzese *et al.*, 1999; Fadiga *et al.*, 1999; Hashimoto and Rothwell, 1999; Rossini *et al.*, 1999; Hanakawa *et al.*, 2003) and in our own pilot data, it has been shown that kinetic imagery is associated with both an increase in muscle tone and in the excitability of the cortico-spinal pathway. This raises the question as to how such an increase might be produced during KI. Besides M1, several association motor areas such as LPMC, SMA and CMA have direct projections to spinal cord through the internal capsule, adjacent to the 'classic' cortico-spinal path originating in M1 (Luppino *et al.*, 1994; Morecraft *et al.*, 2002). Although it is possible that the descending signals could be generated by the small activation in M1, not all subjects had activation in M1 during KI. Since we did not detect activation in CMA, the remaining possibilities are SMA and LPMC. Both areas could be responsible for this increase: In one hand, SMA is exerting heavier influence on M1 (hence it would be a way the system coordinates motor preparation with execution); on the other hand, LPMC is the region with proportionally larger volume of activation during KI (hence, its influence could be directed towards spinal contacts). At this point we cannot predict which of these areas is responsible for the increase in EMG activation because, in contrast to the elegant studies on SMA (Maier *et al.*, 2002), there is a paucity of information regarding the physiological features of cortico-spinal fibers from LPMC. The increase in muscle tone could bring the system closer to threshold in case the movement is actually performed. This result reinforces the idea of KI as part of a system for motor preparation, as has been suggested (Jeannerod, 1995; Stephan and Frackowiak, 1996; Deiber *et al.*, 1998; Lotze *et al.*, 1999; Toni *et al.*, 2001). In this way, the importance of sensory areas during both execution and kinetic imagery makes sense teleologically, as the obvious proprioceptive input involved during execution seems to be present (albeit attenuated) during kinetic imagery (Lacourse *et al.*, 1999; Naito *et al.*, 2002).

The Network for VI was Biased Towards Visual Areas

During VI, primary motor activation and sensory activation were not present. Consequently, somatosensory influences were absent during this task as were all influences on M1. These differences led the network model associated with VI to be significantly different from both the network subserving E and that for KI. In contrast, the stronger connectivity patterns during visual imagery originated in the occipital areas, a result that is consistent with the supposition that this particular behavior is in fact, a visual task (Kosslyn *et al.*, 1999). Although it is not shown in Figure 3, if the occipital activation were due primarily to the sensory input (since subjects were looking at the numbers in the screen), we would expect OCC connectivity to be present in all three conditions. However in E and KI, OCC connectivity was not relevant to the circuit. We suggest then that the value obtained refers to the backward connection (i.e. a top down phenomenon), rather than to the forward connection. We tested this hypothesis, calculating for this case only, the backward connection between PAR and OCC. Values for this were higher than to forward ones. This suggests two interpretations: (i) the task itself requires the visual perception of the subject's fingers in movement; and/or (ii) since forward connections tend to be more dense than backward connections (Rockland, 1994; Rockland and Van Hoesen, 1994), this represents an example where anatomical connectivity and physiological connectivity are mismatched.

The Networks for the Two Imagery Tasks have Parallels

Even though the networks for VI and KI are so different, they nevertheless share a strong connection from PAR to SMA. This input from PAR was stronger during both imagery conditions than during execution. This strong relationship from PAR to SMA might reflect its important role in motor imagery processing (in both KI and VI) as previously suggested by others (Roland *et al.*, 1980a; Decety *et al.*, 1994; Stephan and Frackowiak, 1996; Crammond, 1997; Gerardin *et al.*, 2000; Jeannerod, 2001), along with its possible role in the generation of visually-guided movements (Picard and Strick, 2003). The fact that the connectivity between PAR and SMA seems particularly relevant during the imagery tasks is extremely interesting in the context of the present work, since it is precisely these connections that we postulate are responsible for the suppression of activation in M1. Both results together, reinforce the importance of this connection in the generation of motor imagery.

Supplementary Material

Supplementary material can be found at:
http://www.cercor.oupjournals.org/

Notes

We want to thank Dr A.R. McIntosh for his valuable comments and generous assistance, Mr Robert Lyons for technical help in performing the scan sessions and Mr J. Skipper for his help in analysis. The present work was supported by R01-NS-37195 to S.L.S. and NIH MH 01916 to A.S.

Address correspondence to Ana Solodkin, Department of Neurology, The University of Chicago, MC 2030, 5841 South Maryland Ave, Chicago, IL 60637, USA. Email: solodkin@uchicago.edu.

References

Abbruzzese G, Assini A, Buccolieri A, Marchese R, Trompetto C (1999) Changes of intracortical inhibition during motor imagery in human subjects. Neurosci Lett 263:113–116.

Arbuckle JL (1989) Analysis of moment structures. Am Stat 43:66–67.

Attwell, D and Iadecola, C (2002) The neural basis of functional brain imaging signals. Trends Neurosci 25:621–625.

Bandettini PA, Jesmanowicz A, Wong EC, Hyde JS (1993) Processing strategies for time-course data sets in functional MRI of the human brain. Magn Reson Med 30:161–173.

Beisteiner R, Hollinger P, Lindinger G, Lang W, Berthoz A (1995) Mental representations of movements. Brain potentials associated with imagination of hand movements. Electroencephalogr Clin Neurophysiol 96:183–193.

Binder JR, Rao SM (1995) Human brain mapping and functional magnetic resonance imaging. In: Localization and neuroimaging in neuropsychology (Kertesz A, ed.), pp. 185–212. Orlando, FL: Academic Press.

Binkofski F, Amunts K, Stephan KM, Posse S, Schormann T, Freund HJ, Zilles K, Seitz RJ (2000) Broca's region subserves imagery of motion: a combined cytoarchitectonic and fMRI study. Hum Brain Mapp 11:273–285.

Buchel C, Friston K (2000) Assessing interactions among neuronal systems using functional neuroimaging. Neural Netw 13:871–882.

Buchel C, Friston KJ (1997) Modulation of connectivity in visual pathways by attention: cortical interactions evaluated with structural equation modelling and fMRI. Cereb Cortex 7:768–778.

Cohen JD, MacWhinney B, Flatt M, Provost J (1993) PsyScope: a new graphic interactive environment for designing psychology experiments. Behav Res Meth Inst Comp 25:257–271.

Crammond DJ (1997) Motor imagery: never in your wildest dream. Trends Neurosci 20:54–57.

Decety J, Jeannerod M (1995) Imagery and its neurological substrate. Rev Neurol (Paris) 151:474–479.

Decety J, Jeannerod M, Germain M, Pastene J (1991) Vegetative response during imagined movement is proportional to mental effort. Behav Brain Res 42:1–5.

Decety J, Perani D, Jeannerod M, Bettinardi V, Tadary B, Woods R, Mazziotta JC, Fazio F (1994) Mapping motor representations with positron emission tomography. Nature 371:600–602.

Deiber MP, Ibanez V, Honda M, Sadato N, Raman R, Hallett M (1998) Cerebral processes related to visuomotor imagery and generation of simple finger movements studied with positron emission tomography. Neuroimage 7:73–85.

Fadiga L, Buccino G, Craighero L, Fogassi L, Gallese V, Pavesi G (1999) Corticospinal excitability is specifically modulated by motor imagery: a magnetic stimulation study. Neuropsychologia 37:147–158.

Forman SD, Cohen JD, Fitzgerald M, Eddy WF, Mintun MA, Noll DC (1995) Improved assessment of significant change in functional magnetic resonance imaging (fMRI): use of a cluster size threshold. Magn Reson Med 33:636–647.

Gerardin E, Sirigu A, Lehericy S, Poline JB, Gaymard B, Marsault C, Agid Y, Le Bihan D (2000) Partially overlapping neural networks for real and imagined hand movements. Cereb Cortex 10:1093–1104.

Gonzalez-Lima F, McIntosh AR (1994) Neural network interactions related to auditory learning analyzed with structural equation modelling. Hum Brain Mapp 2:23–44.

Hallett M, Fieldman J, Cohen LG, Sadato N, Pascual-Leone A (1994) Involvement of primary motor cortex in motor imagery and mental practice. Behav Brain Sci 17:210.

Hanakawa T, Immisch I, Toma K, Dimyan MA, Van Gelderen P, Hallett M (2003) Functional properties of brain areas associated with motor execution and imagery. J Neurophysiol 89:989–1002.

Hashimoto R, Rothwell JC (1999) Dynamic changes in corticospinal excitability during motor imagery. Exp Brain Res 125:75–81.

Horwitz B, Friston KJ, Taylor JG (2000) Neural modeling and functional brain imaging: an overview. Neural Netw 13:829–846.

Jeannerod M (1995) Mental imagery in the motor context. Neuropsychologia 33:1419–1432.

Jeannerod M (2001) Neural simulation of action: a unifying mechanism for motor cognition. Neuroimage 14:S103–109.

Kim SG, Jennings JE, Strupp JP, Andersen P, Ugurbil K (1995) Functional MRI of human motor cortices during overt and imagined finger movements. Int J Imag Sys Technol 6:271–279.

Kohler S, McIntosh AR, Moscovitch M, Winocur G (1998) Functional interactions between the medial temporal lobes and posterior neocortex related to episodic memory retrieval. Cereb Cortex 8:451–461.

Kosslyn SM, Pascual-Leone A, Felician O, Camposano S, Keenan JP, Thompson WL, Ganis G, Sukel KE, Alpert NM (1999) The role of area 17 in visual imagery: convergent evidence from PET and rTMS. Science 284:167–170.

Lacourse MG, Cohen MJ, Lawrence KE, Romero DH (1999) Cortical potentials during imagined movements in individuals with chronic spinal cord injuries. Behav Brain Res 104:73–88.

Lotze M, Montoya P, Erb M, Hulsmann E, Flor H, Klose U, Birbaumer N, Grodd W (1999) Activation of cortical and cerebellar motor areas during executed and imagined hand movements: an fMRI study. J Cogn Neurosci 11:491–501.

Luppino G, Matelli M, Camarda R, Rizzolatti G (1994) Corticospinal projections from mesial frontal and cingulate areas in the monkey. Neuroreport 5:2545–2548.

McArdle JJ, McDonald RP (1984) Some algebraic principles of the reticular action model for moment structures. Br J Math Stat Psychol 37:234–251.

Machulda MM, Ward HA, Cha R, O'Brien P, Jack CR Jr (2001) Functional inferences vary with the method of analysis in fMRI. Neuroimage 14:1122–1127.

McIntosh AR (1999) Mapping cognition to the brain through neural interactions. Memory 7:523–548.

McIntosh AR (2000) Towards a network theory of cognition. Neural Netw 13:861–870.

McIntosh AR, Gonzalez-Lima F (1992) Structural modeling of functional visual pathways mapped with 2-deoxyglucose: effects of patterned light and footshock. Brain Res 578:75–86.

McIntosh AR, Gonzalez-Lima F (1994) Structural equation modelling and its application to network analysis in functional brain imaging. Hum Brain Mapp 2:2–22.

McIntosh AR, Gonzalez-Lima F (1998) Large-scale functional connectivity in associative learning: interrelations of the rat auditory, visual, and limbic systems. J Neurophysiol 80:3148–3162.

McIntosh AR, Grady CL, Ungerleider LG, Haxby JV, Rapoport SI, Horwitz B (1994) Network analysis of cortical visual pathways mapped with PET. J Neurosci 14:655–666.

McIntosh AR, Fitzpatrick SM, Friston KJ (2001) On the marriage of cognition and neuroscience. Neuroimage 14:1231–1237.

Maier MA, Armand J, Kirkwood PA, Yang HW, Davis JN, Lemon RN (2002) Differences in the corticospinal projection from primary motor cortex and supplementary motor area to macaque upper limb motoneurons: an anatomical and electrophysiological study. Cereb Cortex 12:281–296.

Morecraft RJ, Herrick JL, Stilwell-Morecraft KS, Louie JL, Schroeder CM, Ottenbacher JG, Schoolfield MW (2002) Localization of arm representation in the corona radiata and internal capsule in the non-human primate. Brain 125:176–198.

Naito E, Kochiyama T, Kitada R, Nakamura S, Matsumura M, Yonekura Y, Sadato N (2002) Internally simulated movement sensations during motor imagery activate cortical motor areas and the cerebellum. J Neurosci 22:3683–3691.

Noll DC, Cohen JD, Meyer CH, Schneider W (1995) Spiral K-space MRI of cortical activation. J Magn Reson Imaging 5:49–56.

Nyberg L, McIntosh AR, Cabeza R, Nilsson LG, Houle S, Habib R, Tulving E (1996) Network analysis of positron emission tomography regional cerebral blood flow data: ensemble inhibition during episodic memory retrieval. J Neurosci 16:3753–3759.

Oishi K, Kimura M, Yasukawa M, Yoneda T, Maeshima T (1994) Amplitude reduction of H-reflex during mental movement simulation in elite athletes. Behav Brain Res 62:55–61.

Oishi K, Kasai T, Maeshima T (2000) Autonomic response specificity during motor imagery. J Physiol Anthropol Appl Hum Sci 19:255–261.

Oldfield RC (1971) The assessment and analysis of handedness: the Edinburgh Inventory. Neuropsychologia 9:97–113.

Paus T, Otaky N, Caramanos Z, MacDonald D, Zijdenbos A, D'Avirro D, Gutmans D, Holmes C, Tomaiuolo F, Evans AC (1996) *In vivo* morphometry of the intrasulcal gray matter in the human cingulate, paracingulate, and superior-rostral sulci: hemispheric asymmetries, gender differences and probability maps. J Comp Neurol 376:664–673.

Picard N, Strick PL (2003) Activation of the supplementary motor area (SMA) during performance of visually guided movements. Cereb Cortex 13:977–986.

Porro CA, Francescato MP, Cettolo V, Diamond ME, Baraldi P, Zuiani C, Bazzocchi M, di Prampero PE (1996) Primary motor and sensory cortex activation during motor performance and motor imagery: a functional magnetic resonance imaging study. J Neurosci 16:7688–7698.

Rademacher J, Burgel U, Geyer S, Schormann T, Schleicher A, Freund HJ, Zilles K (2001) Variability and asymmetry in the human precentral motor system. A cytoarchitectonic and myeloarchitectonic brain mapping study. Brain 124:2232–2258.

Rademacher J, Burgel U, Zilles K (2002) Stereotaxic localization, intersubject variability, and interhemispheric differences of the human auditory thalamocortical system. Neuroimage 17:142–160.

Rockland KS (1994) The organization of feedback connections from area V2 (18) to V1 (17). In: Cerebral cortex (Peters A, Rockland KS, eds), pp. 261–299. New York: Plenum Press.

Rockland KS, Van Hoesen GW (1994) Direct temporal-occipital feedback connections to striate cortex (V1) in the macaque monkey. Cereb Cortex 4:300–313.

Roland PE, Larsen B, Lassen NA, Skinhj E (1980a) Supplementary motor area and other cortical areas in organization of voluntary movements in man. J Neurophysiol 43:118–136.

Roland PE, Skinhoj E, Lassen NA, Larsen B (1980b) Different cortical areas in man in organization of voluntary movements in extrapersonal space. J Neurophysiol 43:137–150.

Rossini PM, Rossi S, Pasqualetti P, Tecchio F (1999) Corticospinal excitability modulation to hand muscles during movement imagery. Cereb Cortex 9:161–167.

Ryding E, Decety J, Sjoholm H, Stenberg G, Ingvar DH (1993) Motor imagery activates the cerebellum regionally. A SPECT rCBF study with 99mTc-HMPAO., Brain Res Cogn Brain Res 1:94–99.

Sanes JN (1994) Neurophysiology of preparation, movement and imagery. Behav Brain Sci 17:221–223.

Solodkin A, Hlustik P, Noll DC, Small SL (2001) Lateralization of motor circuits and handedness during finger movements. Eur J Neurol 8:425–434.

Stephan KM, Frackowiak RS (1996) Motor imagery – anatomical representation and electrophysiological characteristics. Neurochem Res 21:1105–1116.

Talairach J, Tournoux P (1988) Co-planar stereotaxic atlas of the human brain: 3D proportional system: an approach to cerebral imaging. New York: Georg Thieme.

Taylor JG, Krause B, Shah NJ, Horwitz B, Mueller-Gaertner HW (2000) On the relation between brain images and brain neural networks. Hum Brain Mapp 9:165–182.

Toni I, Thoenissen D, Zilles K (2001) Movement preparation and motor intention. Neuroimage 14:S110–S117.

Vanduffel W, Payne BR, Lomber SG, Orban GA (1997) Functional impact of cerebral connections. Proc Natl Acad Sci USA 94:7617–7620.

Waldvogel D, van Gelderen P, Muellbacher W, Ziemann U, Immisch I, Hallett M (2000) The relative metabolic demand of inhibition and excitation. Nature 406:995–998.

Warner L, McNeill ME (1988) Mental imagery and its potential for physical therapy. Phys Ther 68:516–521.

Yaguez L, Nagel D, Hoffman H, Canavan AG, Wist E, Homberg V (1998) A mental route to motor learning: improving trajectorial kinematics through imagery training. Behav Brain Res 90:95–106.

Yaguez L, Canavan AG, Lange HW, Homberg V (1999) Motor learning by imagery is differentially affected in Parkinson's and Huntington's diseases. Behav Brain Res 102:115–127.